
Node Embeddings via Neighbor Embeddings

Jan Niklas Böhm^{*1} Marius Keute^{*1} Alica Guzmán¹ Sebastian Damrich¹ Andrew Draganov²
Dmitry Kobak¹

Abstract

Graph layouts and node embeddings are two distinct paradigms for non-parametric graph representation learning. In the former, nodes are embedded into 2D space for visualization purposes. In the latter, nodes are embedded into a high-dimensional vector space for downstream processing. State-of-the-art algorithms for these two paradigms, force-directed layouts and random-walk-based contrastive learning (such as DeepWalk and node2vec), have little in common. In this work, we show that both paradigms can be approached with a single coherent framework based on established neighbor embedding methods. Specifically, we introduce *graph t-SNE*, a neighbor embedding method for two-dimensional graph layouts, and *graph CNE*, a contrastive neighbor embedding method that produces high-dimensional node representations by optimizing the InfoNCE objective. We show that both graph *t-SNE* and graph *CNE* strongly outperform state-of-the-art algorithms in terms of local structure preservation, while being conceptually simpler.

1. Introduction

Many real-world datasets, ranging from molecule structures to citation networks, come in the form of graphs. Graphs are abstract objects consisting of a set of nodes \mathcal{V} and a set of edges \mathcal{E} which do not inherently belong to any specific metric space. Therefore, the field of graph representation learning has emerged with the goal of embedding the nodes into a metric space \mathbb{R}^d so that neighborhoods are well-preserved. Traditionally, a distinction has been made between (i) *graph layout* (or graph drawing) methods which embed nodes into \mathbb{R}^2 for visualization purposes and (ii) *node embedding* methods like DeepWalk (Perozzi et al.,

2014) and node2vec (Grover & Leskovec, 2016) which embed nodes into higher-dimensional spaces more suitable for downstream analysis, such as classification or clustering. Graph layout methods typically obtain the embeddings by pulling together connected nodes, whereas node embedding methods are typically based on contrastive learning and random-walk notions of node similarity. Both approaches are *non-parametric* and do not require any node features.

Recent work has revealed connections between graph layouts and dimensionality reduction techniques like *t-SNE* (van der Maaten & Hinton, 2008), leading to improved graph layout algorithms (Kruiger et al., 2017; Pitsianis et al., 2019; Zhu et al., 2020a; Zhong et al., 2023). Concurrently, researchers have unified various dimensionality reduction algorithms based on the idea of embedding high-dimensional neighbors near each other (Damrich & Hamprecht, 2021; Böhm et al., 2022) and established connections between neighbor embeddings and contrastive learning (Damrich et al., 2023; Böhm et al., 2023; Hu et al., 2023). This led to implementations that allow optimizing neighbor embeddings in high-dimensional embedding spaces (McInnes et al., 2018; Damrich et al., 2023). Despite these links between graph layouts, data visualization, and contrastive learning, state-of-the-art 2D and high-D graph representation methods remain fundamentally distinct, overlooking the potential of these theoretical connections. This raises a natural question: is there a single, principled approach which unifies these seemingly disparate methods while also achieving competitive performance across both domains, 2D graph layouts and high-D node embeddings?

In this work, we show that such an approach indeed exists. First, we introduce a neighbor-embedding-based graph layout algorithm, *graph t-SNE* (Figure 1), and show that it performs better than existing methods. Second, we introduce a contrastive neighbor embedding algorithm for node embeddings, *graph CNE* (Figure 1), and show that it outperforms DeepWalk and node2vec while being conceptually simpler and without requiring costly hyperparameter tuning. Importantly, both of our proposed techniques emerge naturally from the same underlying principle of neighbor embeddings, demonstrating that a single set of core ideas can yield state-of-the-art performance across these traditionally separate domains.

^{*}Equal contribution ¹Hertie Institute for AI in Brain Health, University of Tübingen, Germany ²Aarhus University, Denmark. Correspondence to: Jan Niklas Böhm <jan-niklas.boehm@uni-tuebingen.de>, Dmitry Kobak <dmitry.kobak@uni-tuebingen.de>.

Code is available at github.com/berenslab/contrastive-graphs.

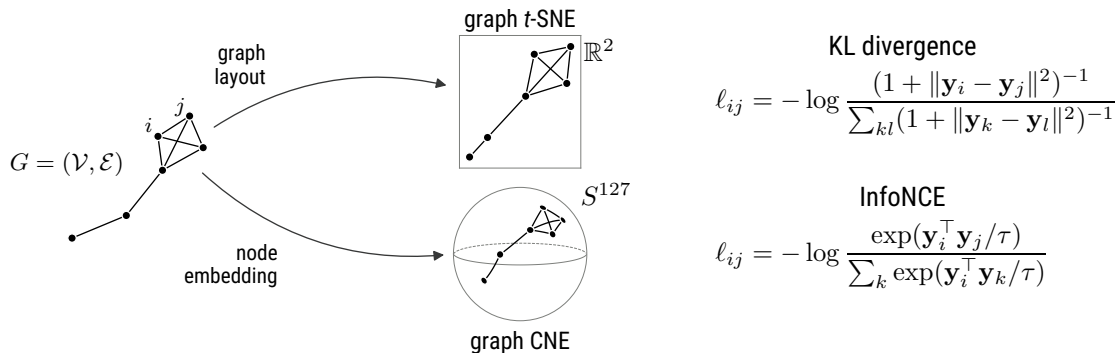


Figure 1. Abstract graph G gets embedded into \mathbb{R}^2 with graph t -SNE or into S^{127} with graph CNE.

2. Related Work

Graph layouts Graph layout algorithms have traditionally been based on spring models, where every connected pair of nodes feels a distance-dependent attractive force F_a and all pairs of nodes feel a distance-dependent repulsive force F_r (*force-directed graph layouts*). Many algorithms can be written as $F_a = d_{ij}^a$ and $F_r = d_{ij}^r$ (Noack, 2007), where d_{ij}^a (resp. d_{ij}^r) is the embedding distance between nodes i and j raised to the a -th (resp. r -th) power. For example, the Fruchterman–Reingold algorithm uses $a = 2, r = -1$ (Fruchterman & Reingold, 1991); ForceAtlas2 uses $a = 1, r = -1$ (Jacomy et al., 2014); LinLog uses $a = 0, r = -1$ (Noack, 2007). Efficient implementations can be based on Barnes–Hut approximation of the repulsive forces, as in SFDP (Hu, 2005). The relationship of ForceAtlas2 to neighbor embeddings was discussed by Böhm et al. (2022).

Several recent graph layout algorithms have been inspired by neighbor embeddings. tsNET (Kruiger et al., 2017) applied a modified version of t -SNE to the pairwise shortest path distances between all nodes. DRGraph (Zhu et al., 2020a) made tsNET faster by using negative sampling (Mikolov et al., 2013). t -FDP (Zhong et al., 2023) suggested custom F_a and F_r forces inspired by t -SNE and adopted the interpolation-based approximation of Linderman et al. (2019). In Section 7.1 we will show that our graph t -SNE outperforms both DRGraph and t -FDP.

SGtSNEpi (Pitsianis et al., 2019) is the closest method to our proposed graph t -SNE algorithm. It applies t -SNE optimization to affinities derived from the graph G , but derives these affinities in a more complex way than we do, and with additional hyperparameters (Section 4.2). In our experiments, our graph t -SNE outperformed SGtSNEpi.

Node embeddings The popular DeepWalk (Perozzi et al., 2014) and node2vec (Grover & Leskovec, 2016) algorithms optimize node placement in a high-dimensional target space based on random walks on graph G . These walks treat nodes as analogous to words and random walk paths as

sentences, enabling the application of word embedding techniques to learn the representation. Specifically, DeepWalk achieves this by performing random walks from each starting node and then using the word2vec algorithm (Mikolov et al., 2013) to ensure that nodes which co-occur often in these random walks are represented near one another in the embedding space. The node2vec algorithm similarly obtains node embeddings by giving graph traversals to the word2vec algorithm, but it differs from DeepWalk by defining two parameters which control the depth-first vs. breadth-first nature of the random walk. These parameters (p and q) provide an additional level of control over the community structure uncovered by the walks, with DeepWalk being a specific instantiation of node2vec when these parameters are both set to 1.

Both DeepWalk and node2vec have been widely adopted for graph-based machine learning applications, including classification and link-prediction tasks (Khosla et al., 2019). Although connections have been drawn between Word2vec and contrastive learning (Arora et al., 2019), we emphasize that the DeepWalk and node2vec algorithms are often regarded as separate from standard contrastive techniques (Grohe, 2020).

Parametric embeddings and node-level graph contrastive learning Our paper is about *non-parametric* embeddings that only use the structure of the graph $G = (\mathcal{V}, \mathcal{E})$. In contrast, *parametric* graph contrastive learning (GCL) methods use node feature vectors and employ a neural network, usually a graph convolutional network (GCN; Kipf & Welling, 2017), to transform features into embedding vectors.

The basic principle behind contrastive learning is to learn data representation by contrasting pairs of observations that are similar to each other (positive pairs) with those that are dissimilar to each other (negative pairs). In computer vision, positive pairs are generated via data augmentation, e.g. in SimCLR (Chen et al., 2020). GCL can be graph-

level or node-level, depending on whether representations are obtained for a set of graphs or for the set of nodes of a single graph. Many graph-level (e.g. You et al., 2020) and node-level GCL algorithms (Velickovic et al., 2019; Zhu et al., 2020b; Hassani & Khasahmadi, 2020; Thakoor et al., 2021; Zhang et al., 2021; Zhu et al., 2021) are also based on graph augmentations, such as node dropping or edge perturbation. A general problem with domain-agnostic graph augmentations is that they can have unpredictable effects on graph semantics (Trivedi et al., 2022). This motivated development of augmentation-free node-level GCL methods, where positive pairs are pairs of nodes that are located close to each other in terms of graph distance (Lee et al., 2022; Li et al., 2023; Zhang et al., 2022). Recent work argued that GCL methods effectively pull connected nodes together, sometimes explicitly through their loss function, but also implicitly through the GCN architecture (Trivedi et al., 2022; Wang et al., 2023; Guo et al., 2023).

Note that Leow et al. (2019) also suggested an algorithm called ‘graph t -SNE’, that uses a GCN to build a parametric mapping optimizing a combination of t -SNE losses on node features and on shortest graph distances; it has almost no relation to our proposed graph t -SNE algorithm, which is non-parametric, and does not use node features or GCNs.

3. Background: Neighbor Embedding Framework

3.1. Neighbor Embeddings

Neighbor embeddings are a family of dimensionality reduction methods aiming to embed n observations from some high-dimensional metric space \mathcal{X} into a lower-dimensional (usually two-dimensional) Euclidean space \mathbb{R}^d , such that neighborhood relationships between observations are preserved in the embedding space. Typically, \mathcal{X} is another real-valued space \mathbb{R}^p , with $d \ll p$. We denote the original vectors as $\mathbf{x}_i \in \mathbb{R}^p$ and the embedding vectors as $\mathbf{y}_i \in \mathbb{R}^d$.

One of the most popular neighbor embedding methods, t -distributed stochastic neighbor embedding (t -SNE; van der Maaten & Hinton, 2008) is an extension of the earlier SNE (Hinton & Roweis, 2002). t -SNE minimizes the Kullback–Leibler divergence between the high-dimensional and low-dimensional *affinities* p_{ij} and q_{ij} :

$$\mathcal{L} = \sum_{ij} p_{ij} \log \frac{p_{ij}}{q_{ij}} = \text{const} - \sum_{ij} p_{ij} \log q_{ij}. \quad (1)$$

Both affinity matrices are defined to be symmetric, positive, and to sum to 1. The high-dimensional affinities \mathbf{P} are computed using adaptive Gaussian kernels such that the distribution of p_{ij} values for any fixed i has a given perplexity (a hyperparameter controlling the effective neighborhood size). Low-dimensional affinities \mathbf{Q} are defined in t -SNE

using a t -distribution kernel with one degree of freedom, also known as the Cauchy kernel:

$$q_{ij} = \frac{(1 + \|\mathbf{y}_i - \mathbf{y}_j\|^2)^{-1}}{\sum_{k \neq l} (1 + \|\mathbf{y}_l - \mathbf{y}_k\|^2)^{-1}}. \quad (2)$$

In practice, t -SNE optimization can be accelerated by an approximation of the repulsive force field based on the Barnes–Hut algorithm (van der Maaten, 2014; Yang et al., 2013), on interpolation (Linderman et al., 2019), or on sampling (Artemenkov & Panov, 2020; Damrich et al., 2023; Draganov et al., 2023; Yang et al., 2023).

3.2. Contrastive Neighbor Embeddings

The contrastive neighbor embedding (CNE) algorithm (Damrich et al., 2023) is a flexible dimensionality reduction framework that replaces t -SNE’s Kullback–Leibler divergence loss with contrastive losses. It considers three different loss functions: NCE (noise-contrastive estimation) (Gutmann & Hyvärinen, 2010), InfoNCE (Jozefowicz et al., 2016; Oord et al., 2018), and negative sampling (Mikolov et al., 2013). These loss functions are called *contrastive* because they are based on contrasting pairs of k -nearest neighbors and non-neighbors in the same mini-batch, and do not require a global normalization like in Equation 2. Using NCE and InfoNCE in CNE approximates t -SNE.

In this work we will only use the InfoNCE loss function. The InfoNCE loss is defined for one pair of k -nearest neighbors ij (*positive pair*) with affinity p_{ij} as

$$\ell(i, j) = -p_{ij} \log \frac{w_{ij}}{w_{ij} + \sum_{k=1}^m w_{ik}}, \quad (3)$$

where w_{ij} are non-normalized low-dimensional affinities and the sum in the denominator is over m *negative pairs* ik where k can be drawn from all points in the same mini-batch apart from i and j . One mini-batch consists of b pairs of neighbors, and hence contains $2b$ points. Therefore, for a given batch size b , the maximal value of m is $2b - 2$. The larger the number of negative samples m , the better is the approximation to t -SNE (Damrich et al., 2023). The InfoNCE loss aims to make w_{ij} large, i.e. place embeddings \mathbf{y}_i and \mathbf{y}_j nearby, if ij is a positive pair, and small if it is a negative one.

The w_{ij} affinities do not need to be normalized. When embedding into \mathbb{R}^2 , they can be defined simply as

$$w_{ij} = (1 + \|\mathbf{y}_i - \mathbf{y}_j\|^2)^{-1}. \quad (4)$$

When using a high-dimensional embedding space, e.g. $d = 128$ instead of $d = 2$, embedding vectors are usually projected to lie on the unit sphere. For points on the unit sphere, the cosine distance and the squared Euclidean

distance differ only by a constant, making the following definitions of w_{ij} equivalent:

$$w_{ij} = \exp(\mathbf{y}_i^\top \mathbf{y}_j / (\|\mathbf{y}_i\| \cdot \|\mathbf{y}_j\|) / \tau) \quad (5)$$

$$= \text{const} \cdot \exp\left(-\left\|\frac{\mathbf{y}_i}{\|\mathbf{y}_i\|} - \frac{\mathbf{y}_j}{\|\mathbf{y}_j\|}\right\|^2 / (2\tau)\right), \quad (6)$$

where τ is called the *temperature* (by default, $\tau = 0.5$). Together with Equation 3, this gives the same loss function as in SimCLR (Chen et al., 2020), a popular contrastive learning algorithm in computer vision. Note that instead of nearest neighbors, SimCLR uses pairs of augmented images as positive pairs.

4. Applying the Neighbor Embedding Framework to Graphs

4.1. General Approach

Standard t -SNE employs Gaussian high-dimensional affinities with most $p_{ij} \approx 0$. This can be seen as a generalization of discrete nearest neighbors: if p_{ij} is close to 0, then the points are effectively dissimilar. However, almost the same visualizations can be obtained using hard nearest neighbors, i.e. simply by normalizing and symmetrizing the k NN graph adjacency matrix \mathbf{A} directly (Böhm et al., 2022):

$$\mathbf{P} = \frac{\mathbf{A}/k + \mathbf{A}^\top/k}{2n}. \quad (7)$$

Here \mathbf{A} has element $a_{ij} = 1$ if \mathbf{x}_j is within the k nearest neighbors of \mathbf{x}_i . Reasonable values of k typically lie between 10 and 100, corresponding to the effective neighborhood size for typical perplexity values.

Similarly, contrastive neighbor embeddings often directly choose the edges of the k NN graph as high-dimensional affinities, $\mathbf{P} = \mathbf{A} / \sum_{ij} A_{ij}$ (Artemenkov & Panov, 2020; Damrich et al., 2023). This is equivalent to simply leaving out p_{ij} from Equation (3).

Thus, even though neither t -SNE nor CNE are usually presented as such, they can be thought of as graph layout algorithms, specifically applied to k NN graphs. During optimization, neighboring nodes (sharing a k NN edge) feel attraction, whereas all nodes feel repulsion, arising through the normalization in Equations 2 and 3.

This suggests a simple strategy for applying the neighbor embedding framework to a general graph G : obtain affinities directly from G instead of a k NN graph of some data, and then run the t -SNE or CNE embedding optimization on these affinities (Figure 1).

4.2. Graph Layouts via Graph t -SNE

Given an unweighted graph $G = (\mathcal{V}, \mathcal{E})$, its adjacency matrix \mathbf{A} has elements $A_{ij} = 1$ if $(i, j) \in \mathcal{E}$ and $A_{ij} = 0$

otherwise. Since all graphs considered in this study are undirected, the adjacency matrix is a binary, symmetric square $n \times n$ matrix. In order to convert it into an affinity matrix suitable for t -SNE, we followed the strategy of Böhm et al. (2022) in Eq. 7: divide each row by the sum of its elements, symmetrize the resulting matrix, and then normalize to sum to 1:

$$\mathbf{P} = \frac{\tilde{\mathbf{A}} + \tilde{\mathbf{A}}^\top}{2n}, \text{ where } \tilde{A}_{ij} = A_{ij} / \sum_{k=1}^n A_{ik}. \quad (8)$$

For optimization, we used `openTSNE` (Poličar et al., 2019) with default parameters. It uses Laplacian Eigenmaps (Belkin & Niyogi, 2003) for initialization (Kobak & Linderman, 2021), sets the learning rate to n to achieve good convergence (Linderman & Steinerberger, 2019; Belkina et al., 2019), and employs the Flt-SNE algorithm that has linear $\mathcal{O}(n)$ runtime (Linderman et al., 2019).

We have also experimented with an alternative way to convert the adjacency matrix into the affinity matrix: namely, to divide \mathbf{A} by the sum of its elements: $\mathbf{P} = \mathbf{A} / \sum_{ij} A_{ij}$. This approach resulted in lower neighbor recall and k NN accuracy values, and gave visually unpleasing embeddings, with low-degree nodes pushed out to the periphery (Figure S2c,f). Furthermore, we experimented with various initialization schemes and found that on our graphs, random initialization performed very similar to the default Laplacian Eigenmaps initialization (Figure S2b,e).

SGtSNEpi (Pitsianis et al., 2019) derives the affinity matrix \mathbf{P} from the adjacency matrix \mathbf{A} in a more complicated way (Pitsianis et al., 2024, Supplementary). Non-zero elements A_{ij} are first weighted by the Jaccard similarity of the sets of neighbors of nodes i and j , then power-transformed to match a pre-specified row sum λ , and finally divided by λ to yield $\tilde{\mathbf{A}}$. By default, $\lambda = 10$.

Table 1. Benchmark datasets. Columns: number of nodes in the largest connected component, number of undirected edges, number of node classes, and the average number of edges per node.

Dataset	Nodes	Edges	Classes	E/N
Citeseer	2 120	7 358	6	3.5
Cora	2 485	10 138	7	4.1
PubMed	19 717	88 648	3	4.5
Photo	7 487	238 086	8	31.8
Computer	13 381	491 556	10	36.7
MNIST k NN	70 000	1 501 392	10	21.4
arXiv	169 343	2 315 598	40	13.7
MAG	726 664	10 778 888	349	14.8

4.3. Node Embeddings via Graph CNE

As in graph t -SNE, graph CNE directly obtains the affinities from a graph G , instead of a k NN graph. Following CNE, we compute them as $\mathbf{P} = \mathbf{A} / \sum_{ij} A_{ij}$. Then, graph CNE optimizes the embedding using a contrastive loss function such as InfoNCE to make neighbors be close in the embedding (Section 3.2).

For all experiments with CNE we used the output dimensionality $d = 128$ and the InfoNCE loss with the cosine distance. We set the batch size to $\min\{8192, |\mathcal{V}|/10\}$ (in pilot experiments we noticed that small graphs required smaller batch sizes for good convergence) and used full-batch repulsion ($m = 2b - 2$). The number of epochs was set to 100. We used the Adam optimizer (Kingma & Ba, 2015) with learning rate 0.001. Graph CNE was initialized with 128-dimensional Laplacian Eigenmaps as well, although, again, there was almost no difference when using random initialization.

Note that our method is conceptually much simpler than DeepWalk and node2vec. In both of these algorithms, random walks are used to implicitly estimate node similarity by their co-occurrence, and then word2vec is employed to train the embedding. Furthermore, node2vec requires per-graph hyperparameter tuning so that its random walk distributions appropriately model the input graph (Grover & Leskovec, 2016). In our graph CNE method, all nodes connected by an edge attract each other, exactly as in graph t -SNE, and no random walks are needed. The main difference between graph t -SNE & CNE is the contrastive loss for efficient optimization in 128 dimensions.

5. Experimental Setup

Datasets We used eight publicly available graph datasets (Table 1). The first five datasets were retrieved from the Deep Graph Library (Wang et al., 2019). The arXiv and MAG dataset were retrieved from the Open Graph Benchmark (Hu et al., 2020). The MNIST k NN dataset was obtained by computing the k NN graph with $k = 15$ on top of the 50 principal components of the MNIST digit dataset (Lecun et al., 1998). Each dataset was treated as an unweighted and undirected graph, where each node has a class label, used only for evaluation. We restricted ourselves to graphs with labeled nodes in order to use classification accuracy as one of the performance metrics. In all datasets we used only the largest connected component and excluded all self-loops if present, using NetworkX (Hagberg et al., 2008) functions `connected_components` and `selfloop_edges`.

Performance metrics We evaluated the performance using three metrics: neighbor recall, k NN classification accu-

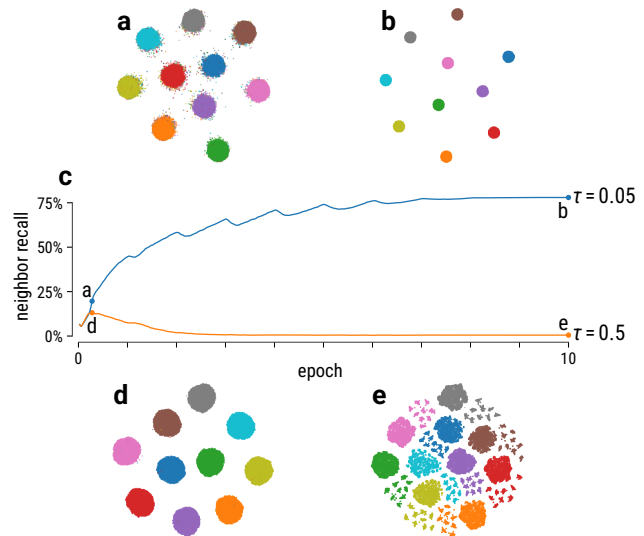


Figure 2. Learning dynamics of the 128-dimensional CNE embeddings of nodes in a stochastic block model graph with 10 blocks. (a, b) t -SNE visualizations of the CNE embeddings with $\tau = 0.05$, in the middle of the first epoch and after ten epochs. (c) The neighbor recall as a function of the training epoch, for $\tau = 0.05$ and for $\tau = 0.5$. Points correspond to t -SNE visualizations above/below. (d, e) Same as (a, b), but for $\tau = 0.5$.

racy, and linear classification accuracy.

The neighbor recall quantifies how well local node neighborhoods are preserved in the embedding. We defined it as the average fraction of each node’s graph neighbors that are among the node’s nearest neighbors in the embedding:

$$\text{Recall} = \frac{1}{|\mathcal{V}|} \sum_{i=1}^{|\mathcal{V}|} \frac{|N_G[i] \cap N_{E,k}[i]|}{k_i}, \quad (9)$$

where $|\mathcal{V}|$ is the number of nodes in the graph, $N_G[i]$ is the set of node i ’s graph neighbors, $N_{E,k}[i]$ denotes the set of node i ’s k Euclidean nearest neighbors in the embedding space, and $k_i = |N_G[i]|$ is the number of node i ’s graph neighbors. This metric does not require ground truth classes and is similar to what is commonly used in the literature to benchmark graph layout algorithms (Kruiger et al., 2017; Zhu et al., 2020a; Zhong et al., 2023). Therefore, we use this as our primary metric for measuring graph layout quality.

The k NN classification accuracy quantifies local class separation in the embedding. To calculate k NN accuracy, we randomly split all nodes into a training (90% of all nodes) and a test set (10%), and used the `KNeighborsClassifier` from scikit-learn with $k = 10$ (Pedregosa et al., 2011).

We used the Euclidean distance to calculate all k NN evaluations (recall and accuracy) in $d = 2$, and the cosine similarity for evaluations in $d = 128$. CNE uses the cosine metric

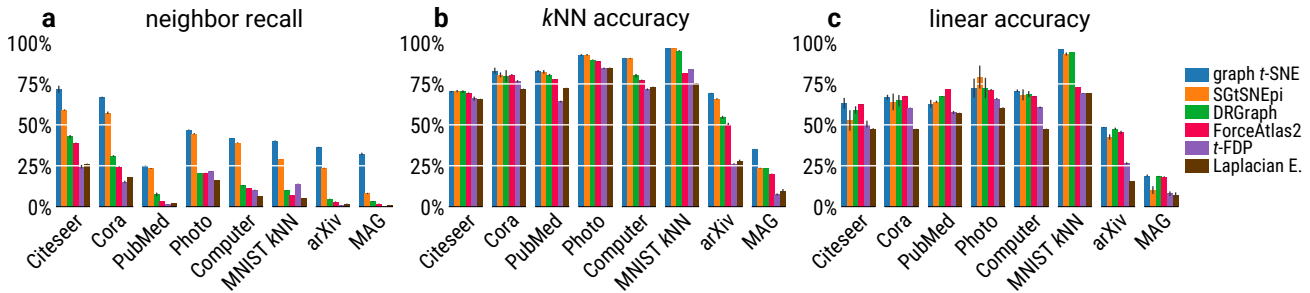


Figure 3. Performance metrics for graph layouts: (a) neighbor recall, (b) k NN accuracy, and (c) linear accuracy. Datasets are ordered by the number of edges. See Figures 5 and S4 for the corresponding layouts.

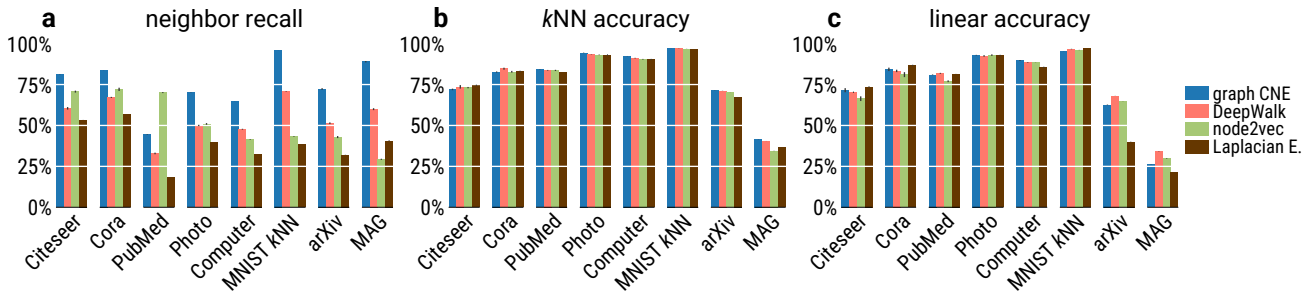


Figure 4. Performance metrics for node embeddings: (a) neighbor recall, (b) k NN accuracy, (c) linear accuracy. Datasets are ordered by the number of edges. For node2vec we did a grid search over $p, q \in \{0.25, 0.5, 1, 2, 4\}$ and show results with the highest neighbor recall.

in its loss function (Equation 6), so only cosine neighbors make sense for evaluation. DeepWalk and node2vec rely on word2vec which uses dot product similarity in the loss function, and the original papers also used cosine metric for evaluation (in our experiments cosine evaluation led to better results on average).

For linear accuracy we used `LogisticRegression` from scikit-learn with no regularization (`penalty=None`), SAGA solver (Defazio et al., 2014) with `tol=0.01`, and the same train/test split. We standardized all features based on the training set.

6. Graph CNE Requires Low Temperature

In pilot experiments, we noticed that the performance of graph CNE was strongly affected by the temperature parameter τ . To investigate it further, we synthesized a graph following the stochastic block model (SBM; Holland et al., 1983). The generated graph had 80 000 nodes in 10 clusters, with any two nodes from the same cluster having probability $2.5 \cdot 10^{-3}$ to be connected by an edge, and any two nodes from two different clusters having probability $5 \cdot 10^{-6}$ to be connected. The resulting graph has a clear community structure that should be easy to recover.

CNE with the default temperature $\tau = 0.5$ achieved near-perfect class separation but failed to retain the neighborhood structure. The neighbor recall, after reaching 13% within the first training epoch, collapsed to below 1% over the next several epochs (Figure 2c, orange line). The t -SNE visualization of the high-dimensional embedding at the point of maximum neighbor recall showed ten compact clusters (Figure 2d), but after convergence it showed nine subclusters for each of the ten classes (Figure 2e). These smaller subclusters corresponded to nodes with an inter-cluster edge to a specific other class. During the optimization, these nodes got ‘pulled out’ of their class, destroying the local structure of the embedding and leading to near-zero neighbor recall.

In contrast, CNE with a lower temperature $\tau = 0.05$ did not show this behavior. The neighbor recall was almost monotonically increasing during training, reaching 78% after 10 epochs (Figure 2c, blue line). The t -SNE visualization showed ten compact clusters (Figure 2b), without any visible subclusters. Our interpretation is that the InfoNCE loss with low temperature could effectively ignore the noise in form of rare inter-class edges.

In the following experiments, we set the temperature of graph CNE to $\tau = 0.05$ for all datasets. We have also implemented learnable temperature, making τ an additional

Table 2. Neighbor recall for all methods and datasets (in %). All values are mean \pm standard deviation across three training runs. The top performing method for each dimensionality is highlighted in bold. Methods in blue are ours.

d	Method	Citeseer	Cora	PubMed	Photo	Computer	MNIST	arXiv	MAG
2	graph t-SNE	71.7 \pm 2.2	66.7 \pm 0.5	25.0 \pm 0.2	46.9 \pm 0.2	41.8 \pm 0.1	40.2 \pm 0.2	36.3 \pm 0.3	32.3 \pm 0.7
	SGtSNEpi	59.1 \pm 0.3	57.4 \pm 0.8	23.3 \pm 0.3	44.5 \pm 0.4	39.0 \pm 0.3	29.1 \pm 0.1	23.6 \pm 0.3	8.1 \pm 0.4
	DRGraph	42.8 \pm 1.0	31.0 \pm 0.5	7.5 \pm 1.1	20.5 \pm 0.1	12.8 \pm 0.4	10.0 \pm 0.1	4.7 \pm 0.2	3.2 \pm 0.3
	ForceAtlas2	38.8 \pm 0.3	24.4 \pm 0.3	3.2 \pm 0.1	20.6 \pm 0.1	11.1 \pm 0.1	7.0 \pm 0.0	2.9 \pm 0.3	1.7 \pm 0.2
	t -FDP	24.4 \pm 1.2	15.2 \pm 0.7	1.3 \pm 0.1	21.6 \pm 0.1	10.2 \pm 0.2	13.9 \pm 0.1	0.7 \pm 0.2	0.3 \pm 0.1
	Laplacian E.	26.2 \pm 0.1	17.9 \pm 0.0	2.0 \pm 0.1	16.0 \pm 0.0	6.4 \pm 0.0	5.0 \pm 0.0	1.6 \pm 0.3	0.8 \pm 0.1
128	graph CNE	81.0 \pm 0.1	83.8 \pm 0.0	44.3 \pm 0.2	70.3 \pm 0.1	64.8 \pm 0.0	96.0 \pm 0.0	72.3 \pm 0.6	89.0 \pm 0.5
	DeepWalk	60.5 \pm 0.9	67.1 \pm 0.4	32.9 \pm 0.6	50.0 \pm 0.5	47.7 \pm 0.3	70.8 \pm 0.2	51.4 \pm 0.6	60.0 \pm 0.7
	node2vec	70.7 \pm 0.6	72.1 \pm 1.0	70.1 \pm 0.3	50.9 \pm 0.5	41.3 \pm 0.2	43.2 \pm 0.2	42.9 \pm 0.6	29.3 \pm 0.4
	Laplacian E.	53.4 \pm 0.0	56.7 \pm 0.0	18.3 \pm 0.1	39.7 \pm 0.0	32.4 \pm 0.0	38.5 \pm 0.0	32.1 \pm 0.1	40.6 \pm 0.3

trainable parameter. We found that on all our benchmark datasets, this the temperature converged towards a value in a range of $[0.04, 0.08]$. The evaluation results were also close to the results with fixed $\tau = 0.05$ (Tables S1 to S3).

7. Benchmarking graph t -SNE and CNE

7.1. Graph t -SNE Outperforms Other Graph Layouts

We compared graph t -SNE with five existing graph layout algorithms: SGtSNEpi (Pitsianis et al., 2019), ForceAtlas2 (FA2; Jacomy et al., 2014), Laplacian Eigenmaps (LE; Belkin & Niyogi, 2003), DRGraph (Zhu et al., 2020a), and t -FDP (Zhong et al., 2023). We did not include tsNET (Kruiger et al., 2017), because it cannot embed large graphs and is outperformed by its successor DRGraph. Unless specified otherwise, we used the original implementation of the algorithms and ran them with the default parameters. For FA2 we used the Barnes–Hut implementation by Chippada (2017). For LE we used scikit-learn, which in turn uses LOBPCG (Knyazev et al., 2007) for solving the generalized eigenproblem. Both t -SNE and t -FDP are implemented in Cython, DRGraph and SGtSNEpi are implemented in C++ and offer wrappers in Python and Julia, respectively. For consistency, we used LE initialization for all algorithms unless not possible (SGtSNEpi and DRGraph).

Graph t -SNE showed outstanding performance on all our benchmark datasets. The neighbor recall of graph t -SNE was always the highest, with SGtSNEpi only sometimes coming close (Figure 3a, Table 2). In terms of k NN accuracy, graph t -SNE was either the top performing method or within 1% of the top performing method for all datasets (Figure 3b, Table S2). In terms of linear accuracy the same was true for six out of the eight datasets (Figure 3c, Table S3). Qualitatively, graph t -SNE layouts did well in terms of separating clusters from each other and bringing out sub-cluster details within individual clusters (Figure 5).

7.2. Graph CNE Outperforms Other Node Embeddings

We compared graph CNE with the popular non-parametric node embedding algorithms DeepWalk (Perozzi et al., 2014) and node2vec (Grover & Leskovec, 2016) (all optimizing 128-dimensional embeddings), as well as with 128-dimensional Laplacian Eigenmaps (LE). We used node2vec’s implementation from PyTorch Geometric (Fey & Lenssen, 2019) and the DeepWalk implementation from DGL (Wang et al., 2019). We ran both methods with the default parameters for 100 epochs (as we did for CNE, see Figure S1 for runtimes). For node2vec, we ran a sweep over the parameters $p, q \in \{0.25, 0.5, 1, 2, 4\}$, as in the original paper, and report the results with the highest neighbor recall (for all results, see Figure S3).

We found that graph CNE outperformed the other algorithms in terms of neighbor recall on seven datasets out of eight; on the PubMed dataset, it was the runner-up (Figure 4a, Table 2). Across all datasets, the average gap in neighbor recall between graph CNE and the best other method was 13.4 percentage points.

In terms of the classification accuracies, the results on most datasets were very similar across all methods including LE. Graph CNE had slightly lower k NN accuracy on the two smallest datasets (Citeseer and Cora), and was the best or within 1% of the best on all other datasets (Figure 4b, Table S2). In terms of linear accuracy, graph CNE yielded competitive results and lagged only slightly behind other methods for some datasets (Figure 4c, Table S3). Curiously, graph CNE with $\tau = 0.5$ was the best or within 1% of the best on all datasets apart from Cora and MAG, where it was slightly behind (Table S3); but this temperature led to substantially worse neighbor recall (Table S1). This suggests a trade-off between linear classification and neighbor quality.

In summary, results in terms of classification accuracies were all similar, but neighbor recall showed large and pronounced differences with graph CNE performing the best.

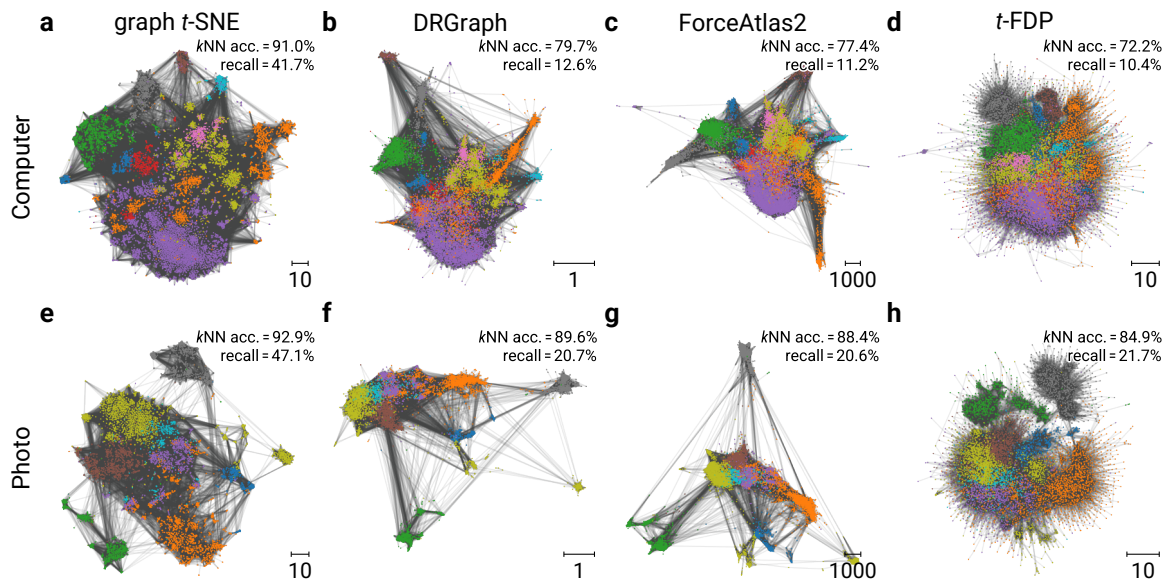


Figure 5. Embeddings of the Computer and Photo dataset obtained using our graph *t*-SNE, DRGraph, ForceAtlas2, and *t*-FDP. Embeddings were aligned using Procrustes rotation. See Figure S4 for all datasets and methods.

8. Discussion

Our paper makes three contributions, two practical and one conceptual. First, we suggested a novel graph layout algorithm, *graph t*-SNE, and showed that it outperforms existing competitors in terms of preserving local graph structure. Second, we suggested a novel node embedding algorithm, *graph CNE*, and showed that it outperforms existing competitors (DeepWalk and node2vec) in terms of preserving local graph structure, while being conceptually simpler and not requiring random walks. Third, we established a *conceptual connection* between 2D graph layouts and high-D node embeddings, and showed that both can be efficiently implemented using existing neighbor embedding frameworks.

Both graph *t*-SNE and graph CNE are remarkably simple, because they use existing *t*-SNE and CNE machinery out of the box. This is in stark contrast with competing algorithms. For example, many existing graph layout algorithms inspired by *t*-SNE, such as tsNET (Kruiger et al., 2017), DRGraph (Zhu et al., 2020a), and *t*-FDP (Zhong et al., 2023), all develop their own machinery, implementation, and approximations, and deviate from *t*-SNE in many different nontrivial ways (see Section 2). SGtSNEpi (Pitsianis et al., 2019) is one exception: it also runs *t*-SNE optimization on graph-derived affinities, however its affinities are more complicated than ours, and our results suggest that this is not needed and is often even detrimental. As we demonstrated, simply applying *t*-SNE optimization to the normalized graph adjacency matrix (i.e. graph *t*-SNE) leads to the best layout quality.

Similarly, graph CNE outperformed both DeepWalk and

node2vec without using any random walks, by simply pulling together connected nodes via contrastive InfoNCE loss function, which is ubiquitous in self-supervised learning in computer vision (Chen et al., 2020) and other domains.

Limitations and future work In this work, we focused on complex real-world graphs and have purposefully not tested our graph *t*-SNE on simple planar graphs or 3D mesh graphs that are often used for benchmarking graph layout algorithms. Such simple graphs are arguably not an interesting case for high-dimensional embeddings, and we aimed to use the same graphs for 2D and high-D benchmarks.

Our work opens up several directions for future work. First, CNE allows to train parametric embeddings (Damrich et al., 2023), which we have not explored here. How would parametric CNE with a GCN mapping compare to existing GCL methods, in particular augmentation-free methods? Second, we only used *t*-SNE here, but a similar approach could be implemented using other neighbor embedding algorithms, e.g. UMAP (McInnes et al., 2018). How would graph UMAP (2D and high-D) perform for graph layouts and node embeddings, especially in contrast to DRgraph and DeepWalk/node2vec, which, like UMAP, use negative sampling for optimization? Third, our results pointed to a non-trivial effect that temperature can have on InfoNCE-based embeddings. Further investigation of this phenomenon and its potential relevance for contrastive learning in computer vision and other domains also remains for future work.

Acknowledgements

The authors would like to thank Leland McInnes and Pavlin Poličar for discussions, and Philipp Berens for support and feedback. The authors benefited from the discussions as the Dagstuhl seminar 24122 supported by the Leibniz Center for Informatics.

This work was partially funded by the Gemeinnützige Hertie-Stiftung, the Cyber Valley Research Fund (D.30.28739), the Danmarks Frie Forskningsfond (Sapere Aude 1051-00106B), and the National Institutes of Health (UM1MH130981). The content is solely the responsibility of the authors and does not necessarily represent the official views of the National Institutes of Health. Dmitry Kobak is a member of the Germany’s Excellence cluster 2064 “Machine Learning — New Perspectives for Science” (EXC 390727645). The authors thank the International Max Planck Research School for Intelligent Systems (IMPRS-IS) for supporting Jan Niklas Böhm.

Impact Statement

The goal of our paper is to advance the field of machine learning. We do not see any potential societal consequences of our work that would be worth specifically highlighting.

References

- Arora, S., Khandeparkar, H., Khodak, M., Plevrakis, O., and Saunshi, N. A theoretical analysis of contrastive unsupervised representation learning. *arXiv preprint arXiv:1902.09229*, 2019.
- Artemenkov, A. and Panov, M. NCVis: noise contrastive approach for scalable visualization. In *Proceedings of The Web Conference 2020*, pp. 2941–2947, 2020.
- Belkin, M. and Niyogi, P. Laplacian eigenmaps for dimensionality reduction and data representation. *Neural Computation*, 15(6):1373–1396, 2003.
- Belkina, A. C., Ciccolella, C. O., Anno, R., Halpert, R., Spidlen, J., and Snyder-Cappione, J. E. Automated optimized parameters for T-distributed stochastic neighbor embedding improve visualization and analysis of large datasets. *Nature Communications*, 10(1):5415, 2019.
- Böhm, J. N., Berens, P., and Kobak, D. Attraction-repulsion spectrum in neighbor embeddings. *The Journal of Machine Learning Research*, 23(1):4118–4149, 2022.
- Böhm, J. N., Berens, P., and Kobak, D. Unsupervised visualization of image datasets using contrastive learning. *International Conference on Learning Representations*, 2023.
- Chen, T., Kornblith, S., Norouzi, M., and Hinton, G. A simple framework for contrastive learning of visual representations. In *International Conference on Machine Learning*, pp. 1597–1607. PMLR, 2020.
- Chippada, B. forceatlas2: Fastest Gephi’s ForceAtlas2 graph layout algorithm implemented for Python and NetworkX. <https://github.com/bhargavchippada/forceatlas2>, 2017.
- Damrich, S. and Hamprecht, F. On UMAP’s true loss function. In *Advances in Neural Information Processing Systems*, 2021.
- Damrich, S., Böhm, N., Hamprecht, F. A., and Kobak, D. From t-SNE to UMAP with contrastive learning. In *The Eleventh International Conference on Learning Representations*, 2023.
- Defazio, A., Bach, F., and Lacoste-Julien, S. SAGA: A fast incremental gradient method with support for non-strongly convex composite objectives. In *Advances in Neural Information Processing Systems*, volume 27, 2014.
- Draganov, A., Jørgensen, J., Scheel, K., Mottin, D., Assent, I., Berry, T., and Aslay, C. Actup: analyzing and consolidating tsne & umap. In *Proceedings of the Thirty-Second International Joint Conference on Artificial Intelligence*, pp. 3651–3658, 2023.
- Fey, M. and Lenssen, J. E. Fast graph representation learning with PyTorch Geometric. In *ICLR Workshop on Representation Learning on Graphs and Manifolds*, 2019.
- Fruchterman, T. M. and Reingold, E. M. Graph drawing by force-directed placement. *Software: Practice and Experience*, 21(11):1129–1164, 1991.
- Grohe, M. word2vec, node2vec, graph2vec, x2vec: Towards a theory of vector embeddings of structured data. In *Proceedings of the 39th ACM SIGMOD-SIGACT-SIGAI Symposium on Principles of Database Systems*, pp. 1–16, 2020.
- Grover, A. and Leskovec, J. node2vec: Scalable feature learning for networks. In *Proceedings of the 22nd ACM SIGKDD International Conference on Knowledge Discovery and Data Mining*, pp. 855–864, 2016.
- Guo, X., Wang, Y., Wei, Z., and Wang, Y. Architecture matters: Uncovering implicit mechanisms in graph contrastive learning. In *Thirty-seventh Conference on Neural Information Processing Systems*, 2023.
- Gutmann, M. and Hyvärinen, A. Noise-contrastive estimation: A new estimation principle for unnormalized statistical models. In *Proceedings of the Thirteenth International*

- Conference on Artificial Intelligence and Statistics*, pp. 297–304. JMLR Workshop and Conference Proceedings, 2010.
- Hagberg, A., Swart, P., and S Chult, D. Exploring network structure, dynamics, and function using NetworkX. Technical report, Los Alamos National Lab, 2008.
- Hassani, K. and Khasahmadi, A. H. Contrastive multi-view representation learning on graphs. In *International Conference on Machine Learning*, pp. 4116–4126. PMLR, 2020.
- Hinton, G. E. and Roweis, S. Stochastic neighbor embedding. *Advances in Neural Information Processing Systems*, 15, 2002.
- Holland, P. W., Laskey, K. B., and Leinhardt, S. Stochastic blockmodels: First steps. *Social Networks*, 5(2):109–137, 1983. ISSN 0378-8733.
- Hu, T., Liu, Z., Zhou, F., Wang, W., and Huang, W. Your contrastive learning is secretly doing stochastic neighbor embedding. *International Conference on Learning Representations*, 2023.
- Hu, W., Fey, M., Zitnik, M., Dong, Y., Ren, H., Liu, B., Catasta, M., and Leskovec, J. Open graph benchmark: Datasets for machine learning on graphs. *Advances in Neural Information Processing Systems*, 33:22118–22133, 2020.
- Hu, Y. Efficient, high-quality force-directed graph drawing. *Mathematica Journal*, 10(1):37–71, 2005.
- Jacomy, M., Venturini, T., Heymann, S., and Bastian, M. ForceAtlas2, a continuous graph layout algorithm for handy network visualization designed for the gephi software. *PloS One*, 9(6):e98679, 2014.
- Jozefowicz, R., Vinyals, O., Schuster, M., Shazeer, N., and Wu, Y. Exploring the limits of language modeling. *arXiv preprint arXiv:1602.02410*, 2016.
- Khosla, M., Setty, V., and Anand, A. A comparative study for unsupervised network representation learning. *IEEE Transactions on Knowledge and Data Engineering*, 33(5):1807–1818, 2019.
- Kingma, D. P. and Ba, J. Adam: A method for stochastic optimization. *International Conference on Learning Representations*, 2015.
- Kipf, T. N. and Welling, M. Semi-supervised classification with graph convolutional networks. *International Conference for Learning Representations*, 2017.
- Knyazev, A. V., Argentati, M. E., Lashuk, I., and Ovtchinnikov, E. E. Block locally optimal preconditioned eigenvalue solvers (blopex) in hypre and petsc. *SIAM Journal on Scientific Computing*, 29(5):2224–2239, 2007.
- Kobak, D. and Linderman, G. C. Initialization is critical for preserving global data structure in both t-SNE and UMAP. *Nature Biotechnology*, 39(2):156–157, 2021.
- Kruiger, J. F., Rauber, P. E., Martins, R. M., Kerren, A., Kobourov, S., and Telea, A. C. Graph layouts by t-SNE. In *Computer Graphics Forum*, volume 36, pp. 283–294. Wiley Online Library, 2017.
- Lecun, Y., Bottou, L., Bengio, Y., and Haffner, P. Gradient-based learning applied to document recognition. *Proceedings of the IEEE*, 86(11):2278–2324, 1998.
- Lee, N., Lee, J., and Park, C. Augmentation-free self-supervised learning on graphs. In *Proceedings of the AAAI Conference on Artificial Intelligence*, volume 36, pp. 7372–7380, 2022.
- Leow, Y. Y., Laurent, T., and Bresson, X. GraphTSNE: a visualization technique for graph-structured data. *Representation Learning on Graphs and Manifold Workshop at the International Conference for Learning Representations*, 2019.
- Li, H., Cao, J., Zhu, J., Luo, Q., He, S., and Wang, X. Augmentation-free graph contrastive learning of invariant-discriminative representations. *IEEE Transactions on Neural Networks and Learning Systems*, pp. 1–11, 2023.
- Linderman, G. C. and Steinerberger, S. Clustering with t-SNE, provably. *SIAM Journal on Mathematics of Data Science*, 1(2):313–332, 2019.
- Linderman, G. C., Rachh, M., Hoskins, J. G., Steinerberger, S., and Kluger, Y. Fast interpolation-based t-SNE for improved visualization of single-cell RNA-seq data. *Nature Methods*, 16(3):243–245, 2019.
- McInnes, L., Healy, J., and Melville, J. UMAP: Uniform manifold approximation and projection for dimension reduction. *arXiv preprint arXiv:1802.03426*, 2018.
- Mikolov, T., Sutskever, I., Chen, K., Corrado, G. S., and Dean, J. Distributed representations of words and phrases and their compositionality. *Advances in Neural Information Processing Systems*, 26, 2013.
- Noack, A. Energy models for graph clustering. *Journal of Graph Algorithms and Applications*, 11(2):453–480, 2007.
- Oord, A. v. d., Li, Y., and Vinyals, O. Representation learning with contrastive predictive coding. *arXiv preprint arXiv:1807.03748*, 2018.

- Pedregosa, F., Varoquaux, G., Gramfort, A., Michel, V., Thirion, B., Grisel, O., Blondel, M., Prettenhofer, P., Weiss, R., Dubourg, V., et al. Scikit-learn: Machine learning in Python. *Journal of Machine Learning Research*, 12:2825–2830, 2011.
- Perozzi, B., Al-Rfou, R., and Skiena, S. Deepwalk: Online learning of social representations. In *Proceedings of the 20th ACM SIGKDD international conference on Knowledge discovery and data mining*, pp. 701–710, 2014.
- Pitsianis, N., Iliopoulos, A.-S., Floros, D., and Sun, X. Spaceland embedding of sparse stochastic graphs. In *2019 IEEE High Performance Extreme Computing Conference (HPEC)*, pp. 1–8, 2019.
- Pitsianis, N., Iliopoulos, A.-S., Floros, D., and Sun, X. Sg-tsne- π . <http://web.archive.org/web/20250124132719/https://t-sne-pi.cs.duke.edu/>, 2024. Accessed: 2025-01-25.
- Poličar, P. G., Stražar, M., and Zupan, B. openTSNE: a modular Python library for t-SNE dimensionality reduction and embedding. *BioRxiv*, pp. 731877, 2019.
- Schönemann, P. H. A generalized solution of the orthogonal procrustes problem. *Psychometrika*, 1966.
- Thakoor, S., Tallec, C., Azar, M. G., Azabou, M., Dyer, E. L., Munos, R., Veličković, P., and Valko, M. Large-scale representation learning on graphs via bootstrapping. *arXiv preprint arXiv:2102.06514*, 2021.
- Trivedi, P., Lubana, E. S., Yan, Y., Yang, Y., and Koutra, D. Augmentations in graph contrastive learning: Current methodological flaws & towards better practices. In *Proceedings of the ACM Web Conference 2022*, pp. 1538–1549, 2022.
- van der Maaten, L. Accelerating t-SNE using tree-based algorithms. *The Journal of Machine Learning Research*, 15(1):3221–3245, 2014.
- van der Maaten, L. and Hinton, G. Visualizing data using t-SNE. *Journal of Machine Learning Research*, 9(11), 2008.
- Veličković, P., Fedus, W., Hamilton, W. L., Liò, P., Bengio, Y., and Devon, R. Deep graph infomax. *International Conference for Learning Representations*, 2(3):4, 2019.
- Wang, M., Zheng, D., Ye, Z., Gan, Q., Li, M., Song, X., Zhou, J., Ma, C., Yu, L., Gai, Y., et al. Deep graph library: A graph-centric, highly-performant package for graph neural networks. *arXiv preprint arXiv:1909.01315*, 2019.
- Wang, Y., Zhang, Q., Du, T., Yang, J., Lin, Z., and Wang, Y. A message passing perspective on learning dynamics of contrastive learning. *International Conference on Learning Representations*, 2023.
- Yang, Z., Peltonen, J., and Kaski, S. Scalable optimization of neighbor embedding for visualization. In *International Conference on Machine Learning*, pp. 127–135. PMLR, 2013.
- Yang, Z., Chen, Y., Sedov, D., Kaski, S., and Corander, J. Stochastic cluster embedding. *Statistics and Computing*, 33(1):12, 2023.
- You, Y., Chen, T., Sui, Y., Chen, T., Wang, Z., and Shen, Y. Graph contrastive learning with augmentations. *Advances in Neural Information Processing Systems*, 33: 5812–5823, 2020.
- Zhang, H., Wu, Q., Yan, J., Wipf, D., and Yu, P. S. From canonical correlation analysis to self-supervised graph neural networks. *Advances in Neural Information Processing Systems*, 34:76–89, 2021.
- Zhang, H., Wu, Q., Wang, Y., Zhang, S., Yan, J., and Yu, P. S. Localized contrastive learning on graphs. *arXiv preprint arXiv:2212.04604*, 2022.
- Zhong, F., Xue, M., Zhang, J., Zhang, F., Ban, R., Deussen, O., and Wang, Y. Force-directed graph layouts revisited: a new force based on the t-distribution. *IEEE Transactions on Visualization and Computer Graphics*, 2023.
- Zhu, M., Chen, W., Hu, Y., Hou, Y., Liu, L., and Zhang, K. DRGraph: An efficient graph layout algorithm for large-scale graphs by dimensionality reduction. *IEEE Transactions on Visualization and Computer Graphics*, 27(2):1666–1676, 2020a.
- Zhu, Y., Xu, Y., Yu, F., Liu, Q., Wu, S., and Wang, L. Deep graph contrastive representation learning. *arXiv preprint arXiv:2006.04131*, 2020b.
- Zhu, Y., Xu, Y., Yu, F., Liu, Q., Wu, S., and Wang, L. Graph contrastive learning with adaptive augmentation. In *Proceedings of the Web Conference 2021*, pp. 2069–2080, 2021.

A. Supplementary Figures and Tables

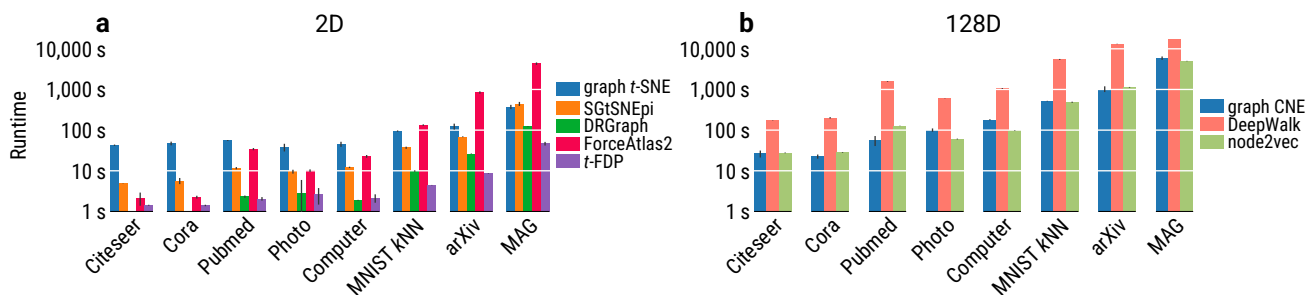


Figure S1. Computation times for graph t -SNE and graph CNE with 2 and 128 output dimensions. All computations were performed on a cluster which isolates the computing resources and removes interference between concurrent computations. All 2D experiments require only CPUs and were ran on 8 cores of an Intel Xeon Gold 6226R. Experiments in 128D ran on a single Nvidia 2080ti GPU card. For node2vec, this shows runtime for $p = 1, q = 1$; we ran 25 parameter combinations, so our actual runtime including hyperparameter tuning was much larger.

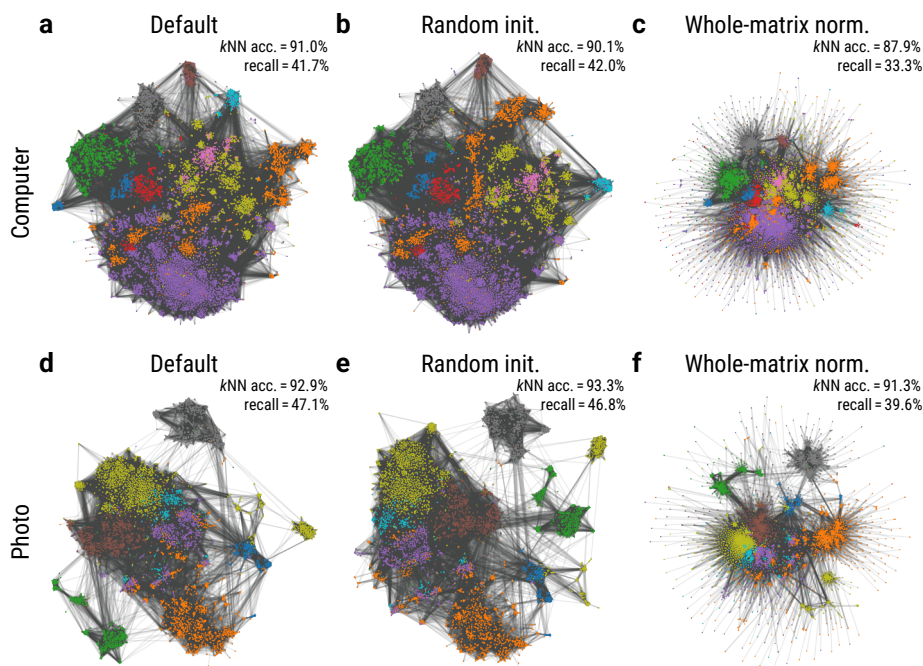


Figure S2. The effect of initialization and normalization on graph t -SNE of Computer and Photo datasets. (a, d) Default graph t -SNE with Laplacian Eigenmaps initialization and using per-node normalization of the adjacency matrix. (b, e) Graph t -SNE using random initialization. (c, f) Graph t -SNE with whole-matrix normalization. Embeddings in each row were aligned using Procrustes rotation.

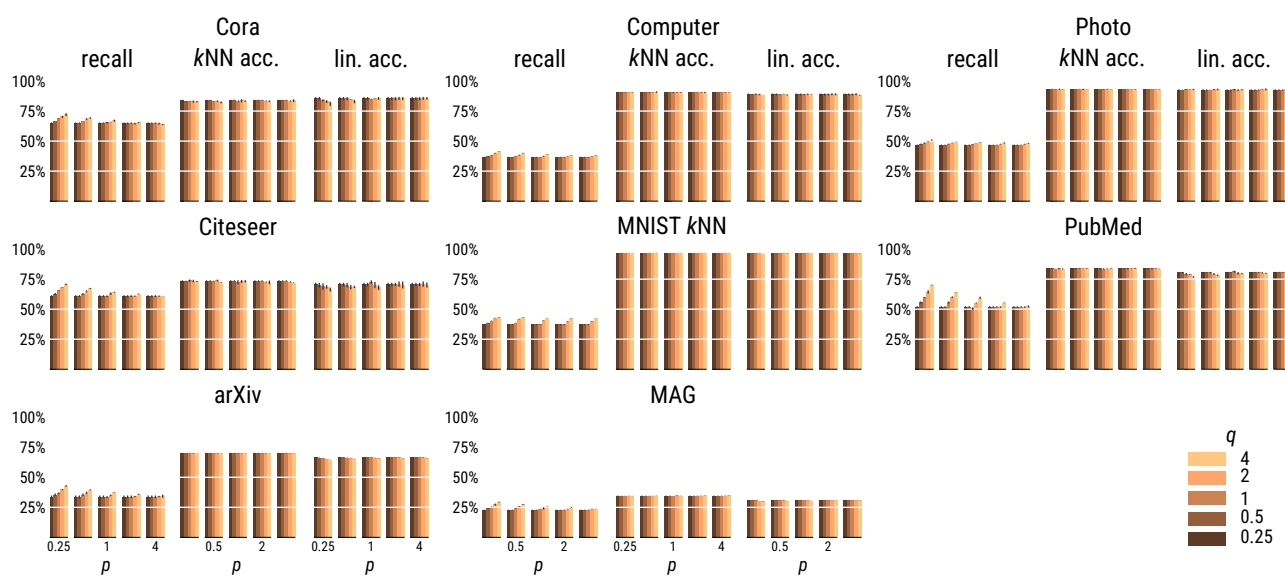


Figure S3. Evaluation for node2vec (Grover & Leskovec, 2016) with the hyperparameters $p, q \in \{0.25, 0.5, 1, 2, 4\}$. These parameter values were taken from the original node2vec paper. The highest neighbor recall was always achieved at $p = 0.25, q = 4$. This corresponds to oversampling unseen nodes.

Node Embeddings via Neighbor Embeddings

Table S1. Neighbor recall for all methods and datasets (in %). All values are mean \pm standard deviation across three training runs and random training/test splits. The top performing method for each dimensionality (and all methods within 1%) is highlighted in bold. Methods in blue are ours. ‘‘Graph CNE τ ’’ means that the temperature τ was learned as a parameter during training, see Section 6.

d	Method	Citeseer	Cora	PubMed	Photo	Computer	MNIST	arXiv	MAG
2	graph t-SNE	71.7 \pm 1.8	66.7 \pm 0.4	25.0 \pm 0.1	46.9 \pm 0.1	41.8 \pm 0.1	40.2 \pm 0.2	36.3 \pm 0.3	32.3 \pm 0.6
	SGtSNEpi	59.1 \pm 0.3	57.4 \pm 0.6	23.3 \pm 0.2	44.5 \pm 0.3	39.0 \pm 0.2	29.1 \pm 0.1	23.6 \pm 0.2	8.1 \pm 0.3
	DRGraph	42.8 \pm 0.8	31.0 \pm 0.4	7.5 \pm 0.9	20.5 \pm 0.1	12.8 \pm 0.3	10.0 \pm 0.1	4.7 \pm 0.1	3.2 \pm 0.2
	ForceAtlas2	38.8 \pm 0.3	24.4 \pm 0.3	3.2 \pm 0.1	20.6 \pm 0.1	11.1 \pm 0.1	7.0 \pm 0.0	2.9 \pm 0.3	1.7 \pm 0.1
	t -FDP	24.4 \pm 0.9	15.2 \pm 0.6	1.3 \pm 0.1	21.6 \pm 0.1	10.2 \pm 0.2	13.9 \pm 0.1	0.7 \pm 0.1	0.3 \pm 0.1
	Laplacian E.	26.2 \pm 0.1	17.9 \pm 0.0	2.0 \pm 0.1	16.0 \pm 0.0	6.4 \pm 0.0	5.0 \pm 0.0	1.6 \pm 0.2	0.8 \pm 0.1
	128	graph CNE	81.0 \pm 0.1	83.8 \pm 0.0	44.3 \pm 0.2	70.3 \pm 0.1	64.8 \pm 0.0	96.0 \pm 0.0	72.3 \pm 0.5
graph CNEτ		80.3 \pm 0.0	82.8 \pm 0.1	42.3 \pm 0.1	69.5 \pm 0.0	64.0 \pm 0.1	96.0 \pm 0.0	72.5 \pm 0.7	91.0 \pm 0.1
CNE, $\tau = 0.5$		55.9 \pm 0.1	58.1 \pm 0.0	21.9 \pm 0.3	35.7 \pm 0.1	31.9 \pm 0.0	39.2 \pm 0.0	34.4 \pm 0.2	33.2 \pm 0.2
DeepWalk		60.5 \pm 0.7	67.1 \pm 0.3	32.9 \pm 0.5	50.0 \pm 0.4	47.7 \pm 0.3	70.8 \pm 0.2	51.4 \pm 0.5	60.0 \pm 0.6
node2vec		70.7 \pm 0.5	72.1 \pm 1.0	70.1 \pm 0.3	50.9 \pm 0.5	41.3 \pm 0.2	43.2 \pm 0.2	42.9 \pm 0.6	29.3 \pm 0.3
Laplacian E.		53.4 \pm 0.0	56.7 \pm 0.0	18.3 \pm 0.1	39.7 \pm 0.0	32.4 \pm 0.0	38.5 \pm 0.0	32.1 \pm 0.1	40.6 \pm 0.2

Table S2. k NN classification accuracy for all methods and datasets (in %). The same setup as in Table S1 applies.

d	Method	Citeseer	Cora	PubMed	Photo	Computer	MNIST	arXiv	MAG
2	graph t-SNE	70.3 \pm 0.4	83.1 \pm 1.5	82.9 \pm 0.5	92.6 \pm 0.5	91.0 \pm 0.0	96.8 \pm 0.1	69.4 \pm 0.2	35.3 \pm 0.0
	SGtSNEpi	70.6 \pm 0.6	80.5 \pm 1.3	82.4 \pm 0.9	92.8 \pm 0.4	90.6 \pm 0.3	96.9 \pm 0.1	65.9 \pm 0.3	23.5 \pm 0.3
	DRGraph	70.3 \pm 0.7	79.8 \pm 2.9	80.4 \pm 0.6	89.8 \pm 0.2	80.1 \pm 0.9	95.2 \pm 0.3	54.7 \pm 0.7	23.3 \pm 0.1
	ForceAtlas2	69.3 \pm 0.4	80.6 \pm 0.3	77.6 \pm 0.2	88.6 \pm 0.2	77.2 \pm 0.4	81.4 \pm 0.0	50.6 \pm 0.6	20.0 \pm 0.2
	t -FDP	66.0 \pm 1.0	76.6 \pm 0.6	64.2 \pm 0.5	84.5 \pm 0.4	71.6 \pm 0.5	83.9 \pm 0.0	26.1 \pm 0.4	7.5 \pm 0.6
	Laplacian E.	65.6 \pm 0.0	71.8 \pm 0.0	72.4 \pm 0.2	84.8 \pm 0.2	73.2 \pm 0.2	75.3 \pm 0.1	27.8 \pm 0.8	9.4 \pm 1.2
	128	graph CNE	72.0 \pm 0.4	82.7 \pm 0.0	84.1 \pm 0.1	94.3 \pm 0.1	92.4 \pm 0.1	97.2 \pm 0.0	71.3 \pm 0.1
graph CNEτ		72.2 \pm 0.4	83.1 \pm 0.3	83.8 \pm 0.3	94.3 \pm 0.1	92.4 \pm 0.2	97.1 \pm 0.0	71.7 \pm 0.1	41.7 \pm 0.1
CNE, $\tau = 0.5$		72.8 \pm 0.2	83.3 \pm 0.2	83.1 \pm 0.0	92.6 \pm 0.0	91.4 \pm 0.0	96.9 \pm 0.0	71.1 \pm 0.1	36.5 \pm 0.1
DeepWalk		73.6 \pm 1.0	84.7 \pm 0.6	83.7 \pm 0.2	93.3 \pm 0.1	91.1 \pm 0.2	97.0 \pm 0.1	71.2 \pm 0.1	40.5 \pm 0.0
node2vec		73.1 \pm 0.4	82.8 \pm 0.5	83.6 \pm 0.4	93.1 \pm 0.2	90.5 \pm 0.2	96.8 \pm 0.0	70.1 \pm 0.0	34.4 \pm 0.1
Laplacian E.		74.5 \pm 0.0	83.1 \pm 0.0	82.6 \pm 0.0	93.0 \pm 0.0	90.3 \pm 0.0	96.7 \pm 0.0	67.2 \pm 0.1	36.5 \pm 0.0

Table S3. Linear classification accuracy for all methods and datasets (in %). The same setup as in Table S1 applies.

d	Method	Citeseer	Cora	PubMed	Photo	Computer	MNIST	arXiv	MAG
2	graph t-SNE	63.2 \pm 2.7	66.9 \pm 1.2	62.8 \pm 2.0	72.5 \pm 4.8	70.9 \pm 0.7	96.0 \pm 0.1	48.4 \pm 0.3	18.9 \pm 0.6
	SGtSNEpi	52.7 \pm 5.2	64.0 \pm 4.2	64.1 \pm 0.5	79.2 \pm 5.8	68.3 \pm 2.8	93.3 \pm 0.7	42.6 \pm 1.4	10.2 \pm 1.9
	DRGraph	59.1 \pm 1.8	64.8 \pm 2.8	67.4 \pm 0.2	72.5 \pm 5.2	68.8 \pm 1.5	94.2 \pm 0.1	47.6 \pm 0.6	18.5 \pm 0.3
	ForceAtlas2	62.4 \pm 0.2	67.3 \pm 0.0	71.6 \pm 0.0	71.4 \pm 0.4	67.3 \pm 0.2	73.1 \pm 0.0	45.4 \pm 0.8	18.2 \pm 0.3
	t -FDP	50.5 \pm 1.7	60.3 \pm 0.2	57.5 \pm 0.8	66.0 \pm 0.4	60.6 \pm 0.5	69.1 \pm 0.2	26.5 \pm 0.5	8.0 \pm 1.1
	Laplacian E.	47.6 \pm 0.0	47.2 \pm 0.0	57.1 \pm 0.0	60.4 \pm 0.0	47.3 \pm 0.0	69.4 \pm 0.0	15.6 \pm 0.0	7.1 \pm 1.4
	128	graph CNE	71.5 \pm 1.2	84.3 \pm 1.0	80.9 \pm 0.2	93.0 \pm 0.2	89.7 \pm 0.2	95.3 \pm 0.0	62.6 \pm 0.2
graph CNEτ		71.9 \pm 1.4	83.6 \pm 0.7	80.2 \pm 0.7	93.4 \pm 0.4	89.5 \pm 0.4	90.8 \pm 0.3	63.6 \pm 0.1	27.6 \pm 0.1
CNE, $\tau = 0.5$		72.8 \pm 0.8	84.3 \pm 0.7	83.6 \pm 0.3	92.7 \pm 0.2	89.4 \pm 0.2	97.1 \pm 0.0	67.9 \pm 0.2	32.2 \pm 0.0
DeepWalk		70.3 \pm 0.0	83.3 \pm 0.7	81.9 \pm 0.3	92.5 \pm 0.4	88.5 \pm 0.2	96.7 \pm 0.1	68.1 \pm 0.0	34.2 \pm 0.1
node2vec		66.4 \pm 1.4	81.0 \pm 1.4	77.0 \pm 0.5	93.0 \pm 0.5	88.5 \pm 0.1	96.1 \pm 0.1	64.6 \pm 0.0	29.9 \pm 0.2
Laplacian E.		73.6 \pm 0.0	86.7 \pm 0.0	81.4 \pm 0.0	92.8 \pm 0.0	85.5 \pm 0.0	97.0 \pm 0.0	40.0 \pm 0.1	21.3 \pm 0.1

Node Embeddings via Neighbor Embeddings

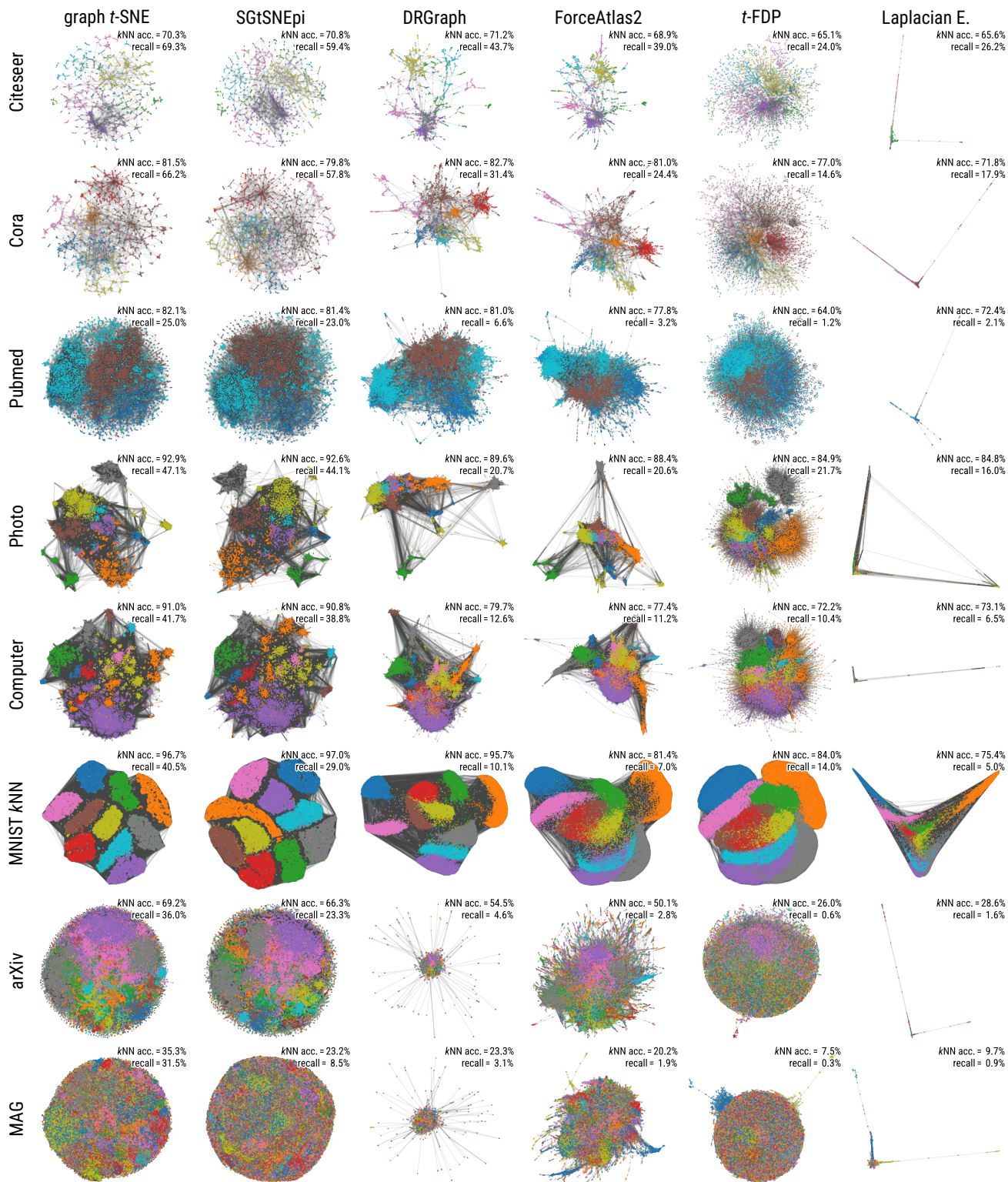


Figure S4. Embeddings of all considered datasets obtained using our graph *t*-SNE, SGtSNEpi (Pitsianis et al., 2019), DRGraph (Zhu et al., 2020a), ForceAtlas2 (Jacomy et al., 2014), *t*-FDP (Zhong et al., 2023), and Laplacian Eigenmaps (Belkin & Niyogi, 2003). Embeddings in each row were aligned using orthogonal Procrustes rotation (Schönemann, 1966).